

Contact interaction probes at the Linear Collider with polarized electron and positron beams¹

A.A. Babich^a, P. Osland^b, A.A. Pankov^{a,c} and N. Paver^c

^a Pavel Sukhoi Technical University, Gomel, 246746 Belarus

^b Department of Physics, University of Bergen,
Allégaten 55, N-5007 Bergen, Norway

^c Dipartimento di Fisica Teorica, Università di Trieste and
Istituto Nazionale di Fisica Nucleare, Sezione di Trieste, Trieste, Italy

Abstract

For contact-interaction searches at the Linear Collider, we discuss the advantages of polarizing both the electron and the positron beams as compared with polarizing only the electron beam. In particular, for the processes $e^+e^- \rightarrow \mu^+\mu^-$, $\tau^+\tau^-$, $b\bar{b}$ and $c\bar{c}$ at a future e^+e^- collider with $\sqrt{s} = 0.5$ TeV we derive model-independent bounds on the four-fermion contact interaction parameters from studies of the helicity cross sections.

¹Partially supported by the Research Council of Norway, and by MURST (Italian Ministry of University, Scientific Research and Technology).

1 Introduction

The possibility of constructing high energy polarized electron and positron beams is considered with great interest with regard to the physics programme at the Linear Collider (LC). Indeed, one of the most important advantages of initial beam polarization is that one can measure spin-dependent observables, which represent the most direct probes of the fermion helicity dependence of the electroweak interactions. Consequently, one would expect a substantial gain in the sensitivity to the features of possible non-standard interactions and, in particular, stringent constraints on the individual new coupling constants could be derived from the data analysis by looking for deviations of cross sections from the Standard Model (SM) predictions.

Here, we will consider the process of fermion pair production ($f \neq e, t$)

$$e^+ + e^- \rightarrow f + \bar{f} \quad (1)$$

at a future Linear Collider with longitudinally polarized electron *and* positron beams, and discuss the sensitivity of the measurable helicity cross sections to the $SU(3) \times SU(2) \times U(1)$ symmetric $eeff$ contact-interaction Lagrangian with helicity-conserving and flavor-diagonal fermion currents [1]:

$$\mathcal{L} = \sum_{\alpha\beta} \frac{g_{\text{eff}}^2}{\Lambda_{\alpha\beta}^2} \eta_{\alpha\beta} (\bar{e}_\alpha \gamma_\mu e_\alpha) (\bar{f}_\beta \gamma^\mu f_\beta). \quad (2)$$

In Eq. (2), generation and color indices have been suppressed, $\alpha, \beta = L, R$ indicate left- or right-handed helicities, and the parameters $\eta_{\alpha\beta} = \pm 1, 0$ specify the chiral structure of the individual interactions. Conventionally, one takes $g_{\text{eff}}^2 = 4\pi$ as a reminder that the new interaction, originally proposed for compositeness, would become strong at $\sqrt{s} \sim \Lambda_{\alpha\beta}$. Actually, in a more general sense, \mathcal{L} should be considered as an effective Lagrangian which represents the leading, lowest dimensional, parameterization at the ‘low-energy’ E at which we make measurements, of some non-standard interaction acting at a much larger energy scale $\Lambda \gg E$. For example, in addition to the remnant compositeness binding force, this is the case of a variety of interactions generated by the exchange of very heavy objects with masses much larger than the Mandelstam variables of the considered process (1), such as the exchanges of a Z' with a few TeV mass [2] and of a heavy leptoquark [3]. In this effective framework, therefore, with the assumed conventional values of η 's and g_{eff}^2 , the scales $\Lambda_{\alpha\beta}$ in Eq. (2) define a standard to compare the reach of different new-physics searches in the process (1).

Clearly, \mathcal{L} should manifest itself by deviations of observables from the SM theoretical predictions. The sensitivity of measurements to the new coupling constants, or, equivalently, the experimentally attainable reach in the free mass scales $\Lambda_{\alpha\beta}$, can be assessed by the numerical comparison of such deviations to the expected experimental accuracies.

For a given flavor f , Eq. (2) defines eight individual, independent models corresponding to the combinations of the four chiralities α, β with the \pm signs of the η 's. However, in general, an observed contact interaction could be any linear combination of these models,

and this leads to the complicated situation in which the aforementioned deviations of observables from the SM predictions simultaneously depend on all four-fermion effective couplings. A simplified, and commonly adopted, procedure is to assume a non-zero value for only one parameter at a time and constrain it by essentially a χ^2 fit analysis, keeping the remaining parameters set equal to zero. In this way, tests of the individual models are obtained.

On the other hand, a general, model-independent, analysis must simultaneously include all terms of Eq. (2) as free parameters and, at the same time, must allow to disentangle their contributions to the basic observables so as to avoid potential cancellations between different contributions. Such cancellations can make the constraints considerably weaker or even spoil them. For this purpose, the longitudinal polarization of initial beams offers the possibility of experimentally separating from the data the individual helicity cross sections of process (1), each one being directly related to a single $eeff$ contact term and, therefore, depending on the minimal set of free independent parameters. The approach we adopt here uses as basic observables two particular, polarized, integrated cross sections that allow to reconstruct the four helicity amplitudes *via* linear combinations of measurements at different beam polarizations.¹ Moreover, in the definition of such integrated observables, optimal kinematical regions can be chosen to maximize the sensitivity to the individual four-fermion contact interactions.

This kind of analysis, and the determination of the corresponding reach on $\Lambda_{\alpha\beta}$, was applied in Ref. [4] for the LC with $\sqrt{s} = 0.5$ TeV and only the electron beam longitudinally polarized, making standard assumptions on the luminosity and on the expected systematic uncertainties on the cross section of process (1) for the different flavors. Indeed, longitudinal polarization of one beam is by itself already sufficient to disentangle the helicity cross sections from the data, if at least two values of the polarization are available, *e.g.*, $\pm|P_e|$. In what follows, we extend the analysis of Ref. [4] and discuss the case where also positron beam longitudinal polarization is available at the LC with the same c.m. energy. Specifically, after giving the main definitions and briefly reviewing the procedure and findings for the sensitivity on $\Lambda_{\alpha\beta}$ obtained in [4], we start by considering the effect of the uncertainty on the electron beam polarization that was disregarded there. We then consider the case of both electron and positron longitudinal polarizations, including in the analysis also the uncertainty on these polarizations.

2 Separation of the helicity cross sections

In Eq. (1) we limit ourselves to the cases $f \neq e, t$ and make the approximation of negligible fermion mass with respect to the c.m. energy \sqrt{s} . Then, the amplitude for $e^+e^- \rightarrow f\bar{f}$ is determined by the Born, s -channel, γ and Z exchanges plus the contact-interaction term of Eq. (2). With P_e and $P_{\bar{e}}$ the longitudinal polarizations of the beams, and θ the angle between the incoming electron and the outgoing fermion in the c.m. frame, the differential

¹Integrated observables should be of advantage in the case of limited experimental statistics.

cross section reads [5]:

$$\frac{d\sigma}{d\cos\theta} = \frac{3}{8} [(1 + \cos\theta)^2\sigma_+ + (1 - \cos\theta)^2\sigma_-]. \quad (3)$$

In terms of helicity cross sections $\sigma_{\alpha\beta}$ (with $\alpha, \beta = \text{L, R}$):

$$\begin{aligned} \sigma_+ &= \frac{1}{4} [(1 - P_e)(1 + P_{\bar{e}})\sigma_{\text{LL}} + (1 + P_e)(1 - P_{\bar{e}})\sigma_{\text{RR}}] \\ &= \frac{D}{4} [(1 - P_{\text{eff}})\sigma_{\text{LL}} + (1 + P_{\text{eff}})\sigma_{\text{RR}}], \end{aligned} \quad (4)$$

$$\begin{aligned} \sigma_- &= \frac{1}{4} [(1 - P_e)(1 + P_{\bar{e}})\sigma_{\text{LR}} + (1 + P_e)(1 - P_{\bar{e}})\sigma_{\text{RL}}] \\ &= \frac{D}{4} [(1 - P_{\text{eff}})\sigma_{\text{LR}} + (1 + P_{\text{eff}})\sigma_{\text{RL}}], \end{aligned} \quad (5)$$

where

$$P_{\text{eff}} = \frac{P_e - P_{\bar{e}}}{1 - P_e P_{\bar{e}}} \quad (6)$$

is the effective polarization [6], $|P_{\text{eff}}| \leq 1$, and $D = 1 - P_e P_{\bar{e}}$. Obviously, for unpolarized positrons $P_{\text{eff}} \rightarrow P_e$ and $D \rightarrow 1$. It should be noted that with $P_{\bar{e}} \neq 0$, $|P_{\text{eff}}|$ can be larger than $|P_e|$. Moreover, in Eqs. (4) and (5):

$$\sigma_{\alpha\beta} = N_C \sigma_{\text{pt}} |A_{\alpha\beta}|^2, \quad (7)$$

where $N_C \approx 3(1 + \alpha_s/\pi)$ for quarks and $N_C = 1$ for leptons, respectively, and $\sigma_{\text{pt}} \equiv \sigma(e^+e^- \rightarrow \gamma^* \rightarrow l^+l^-) = (4\pi\alpha^2)/(3s)$. The helicity amplitudes $A_{\alpha\beta}$ can be written as

$$A_{\alpha\beta} = Q_e Q_f + g_\alpha^e g_\beta^f \chi_Z + \frac{s\eta_{\alpha\beta}}{\alpha\Lambda_{\alpha\beta}^2}, \quad (8)$$

where $\chi_Z = s/(s - M_Z^2 + iM_Z\Gamma_Z)$ is the gauge boson propagator, $g_L^f = (I_{3L}^f - Q_f s_W^2)/s_W c_W$ and $g_R^f = -Q_f s_W^2/s_W c_W$ are the SM left- and right-handed fermion couplings of the Z with $s_W^2 = 1 - c_W^2 \equiv \sin^2\theta_W$ and Q_f the fermion electric charge.

Our analysis focuses on the helicity cross sections that, as the above relations clearly show, directly relate to the individual contact interactions in Eq. (2) with definite chiralities and, accordingly, lead to a model-independent analysis where all terms in this equation are taken into account as completely free parameters with no danger of accidental compensations. To disentangle the various contributions in Eqs. (4) and (5), one simply has to make measurements at two different values of the polarizations (a minimum of four measurements is needed). For example, two convenient sets of values for the polarizations, that we will use in the sequel, would be $P_e = \pm P_1$ and $P_{\bar{e}} = \mp P_2$ ($P_{1,2} > 0$) or, alternatively, $P_{\text{eff}} = \pm P$ and D fixed. The corresponding solutions of Eqs. (4) and (5) read:

$$\sigma_{\text{LL}} = \frac{1}{D} \left[-\frac{1-P}{P}\sigma_+(P) + \frac{1+P}{P}\sigma_+(-P) \right], \quad (9)$$

$$\sigma_{\text{RR}} = \frac{1}{D} \left[\frac{1+P}{P} \sigma_+(P) - \frac{1-P}{P} \sigma_+(-P) \right], \quad (10)$$

with σ_{LR} and σ_{RL} obtained from σ_{LL} and σ_{RR} , respectively, replacing σ_+ by σ_- .

Actually, for the purpose of optimizing the resulting bounds on $\Lambda_{\alpha\beta}$, one can more generally define the polarized cross sections integrated over the *a priori* arbitrary kinematical ranges $(-1, z^*)$ and $(z^*, 1)$ [4]:

$$\sigma_1(z^*, P, D) \equiv \int_{z^*}^1 \frac{d\sigma}{d \cos \theta} d \cos \theta = \frac{1}{8} \{ [8 - (1 + z^*)^3] \sigma_+ + (1 - z^*)^3 \sigma_- \}, \quad (11)$$

$$\sigma_2(z^*, P, D) \equiv \int_{-1}^{z^*} \frac{d\sigma}{d \cos \theta} d \cos \theta = \frac{1}{8} \{ (1 + z^*)^3 \sigma_+ + [8 - (1 - z^*)^3] \sigma_- \}. \quad (12)$$

For simplicity of notations, the polarization dependence of σ_{\pm} on the right-hand sides of Eqs. (11) and (12) has been suppressed. As abbreviations, we introduce

$$a(z^*) = \frac{8 - (1 - z^*)^3}{6(1 - z^{*2})}, \quad b(z^*) = -\frac{(1 - z^*)^3}{6(1 - z^{*2})}. \quad (13)$$

By solving Eqs. (11) and (12) one obtains σ_+ and σ_- from the measurement of σ_1 and σ_2 :

$$\sigma_+ = [a(z^*)\sigma_1(z^*, P, D) + b(z^*)\sigma_2(z^*, P, D)], \quad (14)$$

$$\sigma_- = [b(-z^*)\sigma_1(z^*, P, D) + a(-z^*)\sigma_2(z^*, P, D)]. \quad (15)$$

Thus, according to this procedure, $\sigma_{1,2}(z^*, P, D)$ play the role of a basic set of integrated polarized observables to be measured. As a second step, the corresponding cross sections σ_{\pm} are constructed using the relations (14) and (15) and the experimental values of the helicity cross sections $\sigma_{\alpha\beta}$ are finally determined from the linear system of equations (9)–(10). Moreover, the value of z^* is taken as an input parameter related to given experimental conditions, that can be tuned in order to get maximal sensitivity of the helicity cross sections $\sigma_{\alpha\beta}$ to the mass scales $\Lambda_{\alpha\beta}$ we want to constrain.

For comparison, we recall the conventional observables, the total cross section σ and the various asymmetries. These are generally given, according to Eqs. (3)–(6), by

$$\sigma = \sigma_+ + \sigma_- = \frac{D}{4} [(1 - P_{\text{eff}})(\sigma_{\text{LL}} + \sigma_{\text{LR}}) + (1 + P_{\text{eff}})(\sigma_{\text{RR}} + \sigma_{\text{RL}})]; \quad (16)$$

and

$$\begin{aligned} \sigma A_{\text{FB}} &\equiv \sigma_{\text{F}} - \sigma_{\text{B}} = \frac{3}{4} (\sigma_+ - \sigma_-) \\ &= \frac{3}{16} D [(1 - P_{\text{eff}})(\sigma_{\text{LL}} - \sigma_{\text{LR}}) + (1 + P_{\text{eff}})(\sigma_{\text{RR}} - \sigma_{\text{RL}})]; \end{aligned} \quad (17)$$

with

$$\sigma_{\text{F}} = \sigma_1(z^* = 0) = \int_0^1 (d\sigma/d \cos \theta) d \cos \theta; \quad \sigma_{\text{B}} = \sigma_2(z^* = 0) = \int_{-1}^0 (d\sigma/d \cos \theta) d \cos \theta, \quad (18)$$

and $P_{\text{eff}} \rightarrow 0$, $D \rightarrow 1$ for unpolarized beams. For the case of polarized beams, one has also the left-right asymmetry

$$A_{\text{LR}} = \frac{\sigma_{\text{L}} - \sigma_{\text{R}}}{\sigma_{\text{L}} + \sigma_{\text{R}}} = \frac{(\sigma_{\text{LL}} + \sigma_{\text{LR}}) - (\sigma_{\text{RL}} + \sigma_{\text{RR}})}{\sigma_{\text{LL}} + \sigma_{\text{LR}} + \sigma_{\text{RL}} + \sigma_{\text{RR}}}, \quad (19)$$

and the combined left-right forward-backward asymmetry

$$A_{\text{LR,FB}} = \frac{(\sigma_{\text{L}}^{\text{F}} - \sigma_{\text{R}}^{\text{F}}) - (\sigma_{\text{L}}^{\text{B}} - \sigma_{\text{R}}^{\text{B}})}{(\sigma_{\text{L}}^{\text{F}} + \sigma_{\text{R}}^{\text{F}}) + (\sigma_{\text{L}}^{\text{B}} + \sigma_{\text{R}}^{\text{B}})} = \frac{3}{4} \frac{\sigma_{\text{LL}} - \sigma_{\text{RR}} + \sigma_{\text{RL}} - \sigma_{\text{LR}}}{\sigma_{\text{LL}} + \sigma_{\text{RR}} + \sigma_{\text{RL}} + \sigma_{\text{LR}}}, \quad (20)$$

where σ_{L} and σ_{R} denote the cross sections with left-handed and right-handed electrons and unpolarized positrons.

In the numerical analysis, radiative corrections including initial- and final-state radiation are taken into account by means of the program ZFITTER [7], which has to be used along with ZEFIT, adapted to the present discussion, with $m_{\text{top}} = 175$ GeV and $m_{\text{H}} = 100$ GeV. One-loop SM electroweak corrections are accounted for by improved Born amplitudes [8, 9], such that the form of the previous formulae remains the same. Concerning initial-state radiation, a cut on the energy of the emitted photon $\Delta = E_{\gamma}/E_{\text{beam}} = 0.9$ is applied for $\sqrt{s} = 0.5$ TeV in order to avoid the radiative return to the Z peak, and increase the signal originating from the contact interaction [10].

3 Sensitivity of observables and their optimization

Given the current bounds on $\Lambda_{\alpha\beta}$, of the order of several TeV [11], at the LC c.m. energy $\sqrt{s} = 0.5$ TeV the characteristic suppression factor s/Λ^2 in Eq. (8) is such that we can only look at indirect manifestations of the contact interaction (2) as deviations from the SM predictions. In this case, we can assess the sensitivity of process (1) to the couplings in (2), that determines the corresponding reach on $\Lambda_{\alpha\beta}$, on the basis of the foreseen experimental accuracy on the helicity cross sections $\sigma_{\alpha\beta}$. As stressed previously, the knowledge of the latter allows a model-independent analysis, where all the contact interactions are disentangled and therefore can be taken into account as free parameters simultaneously.

Specifically, we define the ‘significance’ of each helicity cross section by the ratio

$$\mathcal{S}(\sigma_{\alpha\beta}) = \frac{|\Delta\sigma_{\alpha\beta}|}{\delta\sigma_{\alpha\beta}}, \quad (21)$$

where $\Delta\sigma_{\alpha\beta}$ are the deviations from the SM prediction due to (2), dominated for $\sqrt{s} \ll \Lambda_{\alpha\beta}$ by the linear interference term

$$\Delta\sigma_{\alpha\beta} \equiv \sigma_{\alpha\beta} - \sigma_{\alpha\beta}^{\text{SM}} \simeq 2N_{\text{C}} \sigma_{\text{pt}} \left(Q_e Q_f + g_{\alpha}^e g_{\beta}^f \chi_Z \right) \frac{s\eta_{\alpha\beta}}{\alpha\Lambda_{\alpha\beta}^2}, \quad (22)$$

and $\delta\sigma_{\alpha\beta}$ denotes the expected experimental uncertainty on $\sigma_{\alpha\beta}$, combining statistical and systematic uncertainties.

In the procedure of determining helicity amplitudes *via* the integrated polarized cross sections $\sigma_{1,2}$ outlined in the previous section (see Eqs. (9), (10), (14) and (15)), adding all uncertainties in quadrature and neglecting for the moment the systematic uncertainty on the electron and positron polarizations, one can write:

$$\begin{aligned}
(\delta\sigma_{\text{LL}})^2 &= a^2(z^*) \left[\left(\frac{1-P}{PD} \right)^2 (\delta\sigma_1(z^*, P))^2 + \left(\frac{1+P}{PD} \right)^2 (\delta\sigma_1(z^*, -P))^2 \right] \\
&+ b^2(z^*) \left[\left(\frac{1-P}{PD} \right)^2 (\delta\sigma_2(z^*, P))^2 + \left(\frac{1+P}{PD} \right)^2 (\delta\sigma_2(z^*, -P))^2 \right], \quad (23)
\end{aligned}$$

$$\begin{aligned}
(\delta\sigma_{\text{LR}})^2 &= b^2(-z^*) \left[\left(\frac{1-P}{PD} \right)^2 (\delta\sigma_1(z^*, P))^2 + \left(\frac{1+P}{PD} \right)^2 (\delta\sigma_1(z^*, -P))^2 \right] \\
&+ a^2(-z^*) \left[\left(\frac{1-P}{PD} \right)^2 (\delta\sigma_2(z^*, P))^2 + \left(\frac{1+P}{PD} \right)^2 (\delta\sigma_2(z^*, -P))^2 \right], \quad (24)
\end{aligned}$$

where a and b are given by Eq. (13). For simplicity of notations, the dependence of $\delta\sigma_{1,2}$ on D has not been explicitly indicated. One can derive explicit expressions for $\delta\sigma_{\text{RR}}$ and $\delta\sigma_{\text{RL}}$ from $\delta\sigma_{\text{LL}}$ and $\delta\sigma_{\text{LR}}$, respectively, by the replacement in the above equations of $\pm P \rightarrow \mp P$ in $\delta\sigma_i(z^*, \pm P)$ but not in the corresponding prefactors.

Combining in quadrature statistical and systematic uncertainties on $\sigma_{1,2}$, one finds:

$$(\delta\sigma_i)^2 \simeq (\delta\sigma_i^{\text{SM}})^2 = \frac{\sigma_i^{\text{SM}}}{\epsilon \mathcal{L}_{\text{int}}} + (\delta^{\text{sys}} \sigma_i^{\text{SM}})^2, \quad i = 1, 2. \quad (25)$$

For our numerical analysis we shall assume the commonly used reference values of the identification efficiencies, ϵ , and the systematic uncertainties, δ^{sys} , for the various fermionic channels [12]: $\epsilon = 95\%$ and $\delta^{\text{sys}} = 0.5\%$ for l^+l^- ; $\epsilon = 60\%$ and $\delta^{\text{sys}} = 1\%$ for $b\bar{b}$; $\epsilon = 35\%$ and $\delta^{\text{sys}} = 1.5\%$ for $c\bar{c}$. Notice that, as a simplification, we take the same δ^{sys} for both $i = 1$ and 2 , and independent of z^* in the relevant angular range. Concerning the statistical uncertainty, we consider the LC with $\sqrt{s} = 0.5$ TeV, $\mathcal{L}_{\text{int}} = 50 \text{ fb}^{-1}$ and $\mathcal{L}_{\text{int}} = 500 \text{ fb}^{-1}$ (half for each polarization orientation), and a fiducial experimental angular range $|\cos\theta| \leq 0.99$.

Finally, as regards optimization of the bounds on contact-interaction couplings, which corresponds to the maximum value of the ‘significance’ defined in Eq. (21), one may notice from the equations above that the uncertainties $\delta\sigma_{\alpha\beta}$ depend on the, *a priori* free, kinematical parameter z^* in the definition of the polarized cross sections σ_i . Conversely, by definition, the deviations from the SM $\Delta\sigma_{\alpha\beta}$ in Eq. (22) are z^* -independent. Therefore, optimization can be achieved by choosing $z^* = z_{\text{opt}}^*$ where $\delta\sigma_{\alpha\beta}$ becomes minimum, so that the corresponding sensitivity has a maximum and determines the highest bound on the corresponding mass scale $\Lambda_{\alpha\beta}$. The z^* dependence of the statistical uncertainties $\delta\sigma_{\alpha\beta}^{\text{stat}}$ in the right-hand side of (25) can be approximated by that corresponding to the known

SM cross sections for the process (1) and the value of \mathcal{L}_{int} . In the case of low luminosity where the statistical uncertainty dominates, this SM-determined z^* behaviour can be used for a simple, first determination of z_{opt}^* for the various helicity amplitudes [4]. In the general case where statistical and systematic uncertainties are comparable, the optimal z^* must be determined by a more complex numerical analysis taking into account the relevant experimental details.

4 Polarization uncertainty and two polarized beams

In order to assess the effects on the $\delta\sigma_{\alpha\beta}$ due to the systematic uncertainties δP_e and $\delta P_{\bar{e}}$ on the e^- and e^+ polarizations respectively, we must supplement by appropriate terms Eqs. (23) and (24) and the similar ones for the remaining helicity amplitudes. From the formulae in Sec. 2, one can see that finite values of δP_e and $\delta P_{\bar{e}}$ will influence the extraction of the helicity cross sections $\sigma_{\alpha\beta}$ through the prefactors of Eqs. (9), (10), (14) and (15), as well as through the dependence of $\sigma_{1,2}$ on P and D . Clearly, a complete assessment of the latter effect would require detailed knowledge of the structure of the overall systematic uncertainty in terms of the different, individual sources, that is not available at present. For the sake of simplicity, we model the systematic uncertainty by assuming that such an effect can be considered as already included in the systematic uncertainties $\delta\sigma_i^{\text{sys}}$ introduced in Eq. (25), regardless of the values of δP_e and $\delta P_{\bar{e}}$ (and P_e and $P_{\bar{e}}$) considered in our discussion. Then, we treat $\sigma_{1,2}$, P_e and $P_{\bar{e}}$ in Eqs. (9) and (10) as if they were independent measurables, and in this spirit, we combine the additional contribution to the uncertainty, $\delta\sigma_{\alpha\beta}^{\text{pol}}$, again in quadrature with the $\delta\sigma_{\alpha\beta}$ determined from the expressions (23) and (24). Thus:

$$(\delta\sigma_{\alpha\beta})^2 \Rightarrow (\delta\sigma_{\alpha\beta})^2 + \left(\delta\sigma_{\alpha\beta}^{\text{pol}}\right)^2. \quad (26)$$

Under the above assumptions, we obtain

$$\begin{aligned} \left(\delta\sigma_{\text{LL}}^{\text{pol}}\right)^2 &= [f(z^*, P)(1 + P_{\bar{e}}P^2) - f(z^*, -P)(1 - P_{\bar{e}}P^2)]^2 \left(\frac{\delta P_e}{D^2P^2}\right)^2 \\ &+ [f(z^*, P)(1 - P_eP^2) - f(z^*, -P)(1 + P_eP^2)]^2 \left(\frac{\delta P_{\bar{e}}}{D^2P^2}\right)^2, \\ \left(\delta\sigma_{\text{RR}}^{\text{pol}}\right)^2 &= [f(z^*, P)(1 - P_{\bar{e}}P^2) - f(z^*, -P)(1 + P_{\bar{e}}P^2)]^2 \left(\frac{\delta P_e}{D^2P^2}\right)^2 \\ &+ [f(z^*, P)(1 + P_eP^2) - f(z^*, -P)(1 - P_eP^2)]^2 \left(\frac{\delta P_{\bar{e}}}{D^2P^2}\right)^2, \end{aligned} \quad (27)$$

with

$$f(z^*, P) = a(z^*)\sigma_1(z^*, P) + b(z^*)\sigma_2(z^*, P). \quad (28)$$

Furthermore, $\delta\sigma_{LR}^{\text{pol}}$ and $\delta\sigma_{RL}^{\text{pol}}$ are obtained from $\delta\sigma_{LL}^p$ and $\delta\sigma_{RR}^p$, respectively, by substituting $a(z^*) \leftrightarrow b(-z^*)$. Numerically, for explicit assessments of the reach on $\Lambda_{\alpha\beta}$, we shall work out the example of $|P_e| = 0.9$ with $\delta P_e/P_e = 0.5\%$ as currently attainable at the SLC [13], and $|P_{\bar{e}}| = 0.6$ [14]. This corresponds to the effective polarization $P_{\text{eff}} = P = 0.974$ and $D = 1.54$. Clearly, introducing positron polarization may amount to a sort of “noise”, unless its magnitude is known with some precision. Since, at present, information on the achievable precision on the positron polarization is unknown, in our numerical analysis we shall vary $\delta P_{\bar{e}}/P_{\bar{e}}$ in a range up to a few tens of percent.

We start by considering, as a first example, electrons that are polarized, but unpolarized positrons, $(|P_e|, |P_{\bar{e}}|) = (0.9, 0.0)$, and then we discuss the case of both initial beams polarized with $(|P_e|, |P_{\bar{e}}|) = (0.9, 0.6)$. Also, as anticipated, we assume half the total integrated luminosity quoted above for each value of the effective polarization, $P_{\text{eff}} = \pm P$. We focus on the impact of finite polarization uncertainties on the sensitivity of the helicity cross sections $\sigma_{\alpha\beta}$ to the contact interaction (2) and the corresponding reach on the mass scales $\Lambda_{\alpha\beta}$ that, as discussed in the previous section, is determined by the uncertainties $\delta\sigma_{\alpha\beta}$ via Eqs. (21), (22) and (26).

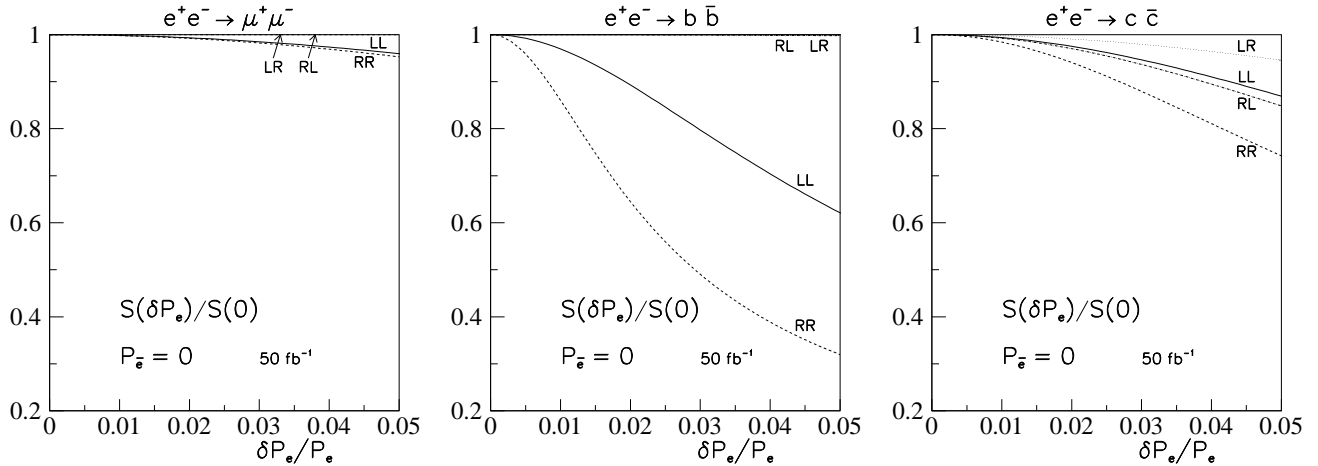


Figure 1: Ratios of sensitivities of helicity cross sections to contact interaction parameters as a function of $\delta P_e/P_e$ compared to no electron polarization uncertainty, for $|P_e| = 0.9$, $|P_{\bar{e}}| = 0.0$ and $\mathcal{L}_{\text{int}} = 50 \text{ fb}^{-1}$. Helicity configurations are indicated.

In the starting example, with polarized electrons and unpolarized positrons, we compare the relative deviations $\delta\sigma_{\alpha\beta}/\sigma_{\alpha\beta} \simeq \delta\sigma_{\alpha\beta}^{\text{SM}}/\sigma_{\alpha\beta}^{\text{SM}}$ for finite δP_e with the case of the same P_e , but $\delta P_e = 0$, studied in [4]. The ratio of the sensitivity (21) in the two cases, determining the effect of the electron polarization uncertainty introduced via Eq. (26), is shown in Fig. 1, for $\mathcal{L}_{\text{int}} = 50 \text{ fb}^{-1}$. This figure is obtained using the optimization procedure, and the determination of the relevant z_{opt}^* , outlined in the previous section. The sensitivity, via its square root, determines the reach in $\Lambda_{\alpha\beta}$. For the $\mu^+\mu^-$ final state, and LL and RR helicity configurations, the effect of δP_e determining $\delta\sigma_{\alpha\beta}^{\text{pol}}$ in (26) is found to change $\delta\sigma_{LL}$ and $\delta\sigma_{RR}$ as given by (23)–(25) and the stated input values by a really modest amount,

of the order of a fraction of a %, unless $\delta P_e/P_e$ exceeds 3–4%, whereas for $\delta\sigma_{LR}$ and $\delta\sigma_{RL}$ there is no change at all. The reason for this can be found in Eqs. (27) and (28). Indeed, within the set of assumptions leading to those equations, one has numerically:

$$\begin{aligned} \left(\delta\sigma_{LL,RR}^{\text{pol}}\right)^2 &\sim [(\sigma_{LL} - \sigma_{RR}) \mp P_e P(\sigma_{LL} + \sigma_{RR})]^2 (\delta P_e)^2 \\ &+ [(\sigma_{LL} - \sigma_{RR}) \pm P_e P(\sigma_{LL} + \sigma_{RR})]^2 (\delta P_e)^2, \end{aligned} \quad (29)$$

independent of z^* , and similar expressions for $\delta\sigma_{LR,RL}^{\text{pol}}$ with the substitutions LL,RR \rightarrow LR,RL. Thus, for $P_e = \delta P_e = 0$, $\delta\sigma_{LL}^{\text{pol}} \sim \delta\sigma_{RR}^{\text{pol}} \sim \sigma_{LL}^{\text{SM}} - \sigma_{RR}^{\text{SM}}$, which for final-state muons vanishes in the limit of $\sin^2\theta_W \rightarrow 0.25$, whereas $\delta\sigma_{LR}^{\text{pol}} \sim \delta\sigma_{RL}^{\text{pol}} \sim \sigma_{LR}^{\text{SM}} - \sigma_{RL}^{\text{SM}} = 0$. It should be stressed that this lack of sensitivity to δP_e depends on having no positron polarization, $P_{\bar{e}} = 0$. For quarks, the corresponding differences of helicity cross sections do not vanish, and the effect of δP_e is to yield a non-zero $\delta\sigma_{\alpha\beta}^{\text{pol}}$. The contribution of δP_e to the helicity cross section uncertainty, $\delta\sigma_{\alpha\beta}^{\text{pol}}$, is still quite small with respect to the total uncertainty, as long as $\delta P_e/P_e$ remains less than 2–3%, except for the LL and RR cases of $b\bar{b}$ final states. For higher luminosity, the curves become steeper, i.e., the sensitivity deteriorates faster

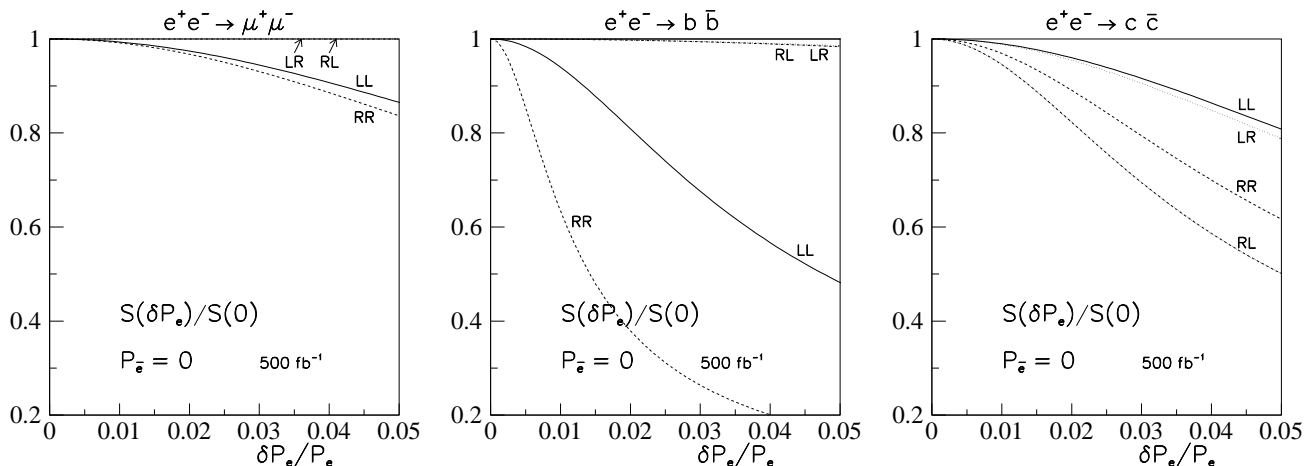


Figure 2: Same as Fig. 1, but for $\mathcal{L}_{\text{int}} = 500 \text{ fb}^{-1}$.

with loss of polarization accuracy, see Fig. 2.

Turning to the case of both positron and electron longitudinal polarization, and referring to Eqs. (4) and (5), in the chosen helicity configuration where $P_e P_{\bar{e}} < 0$, one has $D > 1$ and $|P_{\text{eff}}| > \max(|P_e|, |P_{\bar{e}}|)$, and in principle one could expect on statistical grounds an increase of the sensitivity due to the polarization of positrons, provided the luminosity remains the same. However, this improvement from positron polarization is obtained up to a maximum value of $\delta P_{\bar{e}}/P_{\bar{e}}$, above which there is no benefit, but, actually, a worsening of the sensitivity.

Indeed, it is instructive to compare the sensitivity of the helicity cross sections to four-fermion contact interactions for both beams polarized with that obtained with just

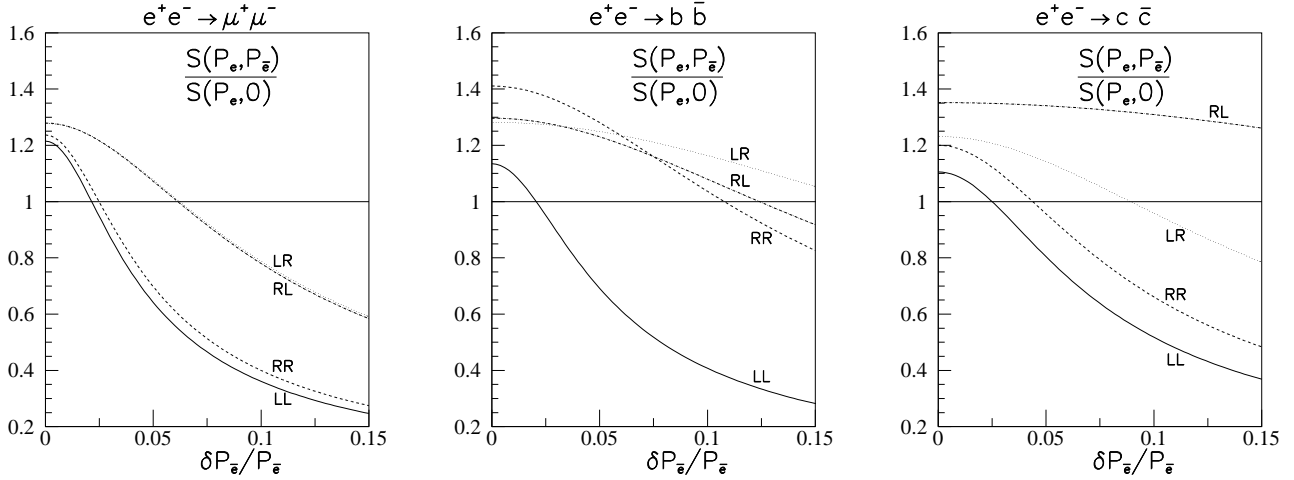


Figure 3: Ratios of sensitivities of helicity cross sections to contact interaction parameters as a function of $\delta P_{\bar{e}}/P_{\bar{e}}$ provided by positron polarization compared to no positron polarization, for $|P_e| = 0.9$, $\delta P_e/P_e = 0.5\%$ and $|P_{\bar{e}}| = 0.6$, $\mathcal{L}_{\text{int}} = 50 \text{ fb}^{-1}$.

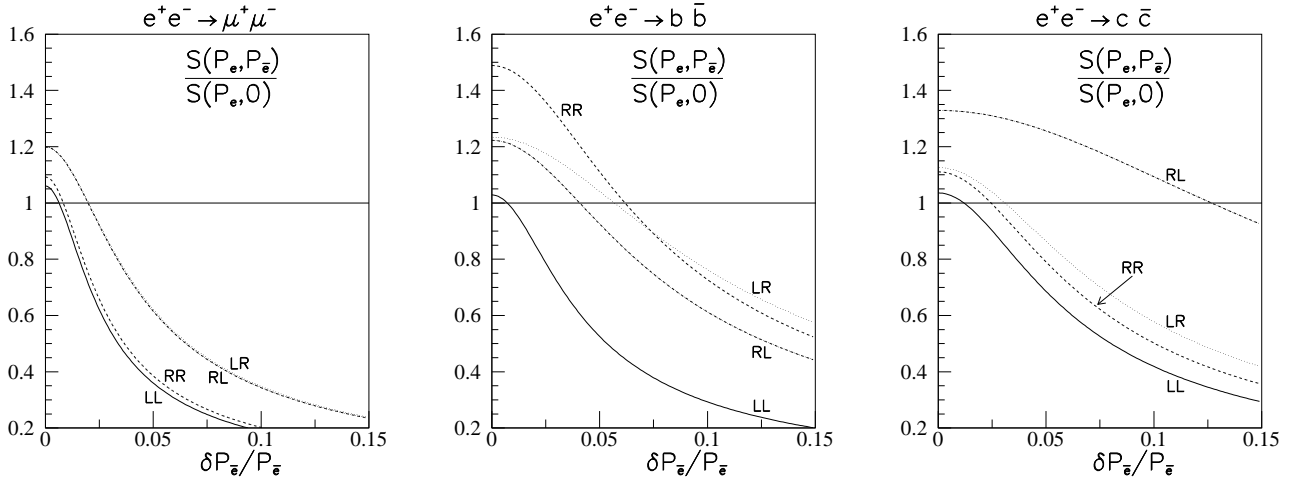


Figure 4: Same as Fig. 3, for $\mathcal{L}_{\text{int}} = 500 \text{ fb}^{-1}$.

one beam polarized. This comparison is expressed in terms of ratios of sensitivities as a function of the positron polarization uncertainty, $\delta P_{\bar{e}}/P_{\bar{e}}$, for $\mathcal{L}_{\text{int}} = 50 \text{ fb}^{-1}$ in Fig. 3 for lepton and quark final states. It is seen that if $|\delta P_{\bar{e}}/P_{\bar{e}}| \approx |\delta P_e/P_e| = 0.5\%$, the advantage of positron polarization manifests itself in an increase in sensitivity by 10–40% depending on the helicity configuration and the final state. However, this ratio drops with increasing $\delta P_{\bar{e}}/P_{\bar{e}}$, and at those positron polarization uncertainties where it becomes less than unity, the advantage of positron polarization disappears. This useful region of the precision $\delta P_{\bar{e}}/P_{\bar{e}}$ ranges from 2% up to beyond 20% depending on the reaction and helicity combination.

This dependence on $\delta P_{\bar{e}}$ can be qualitatively understood from Eq. (29). In the case of

muons (as opposed to quarks), the first term (proportional to $(\delta P_e)^2$) is relatively small (since we consider $P_{\bar{e}}$ considerably less than P_e), and the second term involving $(\delta P_{\bar{e}})^2$ becomes important already at small values of $\delta P_{\bar{e}}$. This explains why the curves (see Fig. 3) are rather steep. Other properties of Fig. 3 are also seen to follow from Eq. (29): (i) for $e^+e^- \rightarrow \mu^+\mu^-$, the dependence on $\delta P_{\bar{e}}$ is the same for the LR and RL cross sections, as well as for the LL and RR ones; (ii) for $e^+e^- \rightarrow b\bar{b}$, the dependence on $\delta P_{\bar{e}}$ is relatively weak for the LR and RL cross sections since these cross sections are small; (iii) for $e^+e^- \rightarrow c\bar{c}$, the dependence on $\delta P_{\bar{e}}$ is much weaker for the RL than for the LR cross section since σ_{LR} is bigger than σ_{RL} , leading to a cancellation in one case and not in the other.

At higher luminosity, all the curves become more steep, since the uncertainty due to the polarization becomes more important w.r.t. the statistical uncertainty. For example, at $\mathcal{L}_{\text{int}} = 500 \text{ fb}^{-1}$, as Fig. 4 shows, for muon final states the positron polarization (at a value $P_{\bar{e}} = 0.6$) stops being useful for the RR and LL cross sections at $\delta P_{\bar{e}}/P_{\bar{e}} = 0.8\%$ and 0.6% , respectively.

In the next section we are going to conclude our numerical discussion by explicitly deriving the reach on the mass scales $\Lambda_{\alpha\beta}$ obtainable in the case where the uncertainty on the electron and positron longitudinal polarizations are, respectively, 0.5% and 1% , for the two values $\mathcal{L}_{\text{int}} = 50 \text{ fb}^{-1}$ and $\mathcal{L}_{\text{int}} = 500 \text{ fb}^{-1}$.

5 Bounds on $\Lambda_{\alpha\beta}$

As a preliminary step in the derivation of the constraints on $\Lambda_{\alpha\beta}$, we show in Fig. 5 the relative uncertainties $\delta\sigma_{\alpha\beta}/\sigma_{\alpha\beta}$ as functions of z^* , for the lower option for the luminosity. The optimal values of z^* where the sensitivity is maximum can be easily read off from these

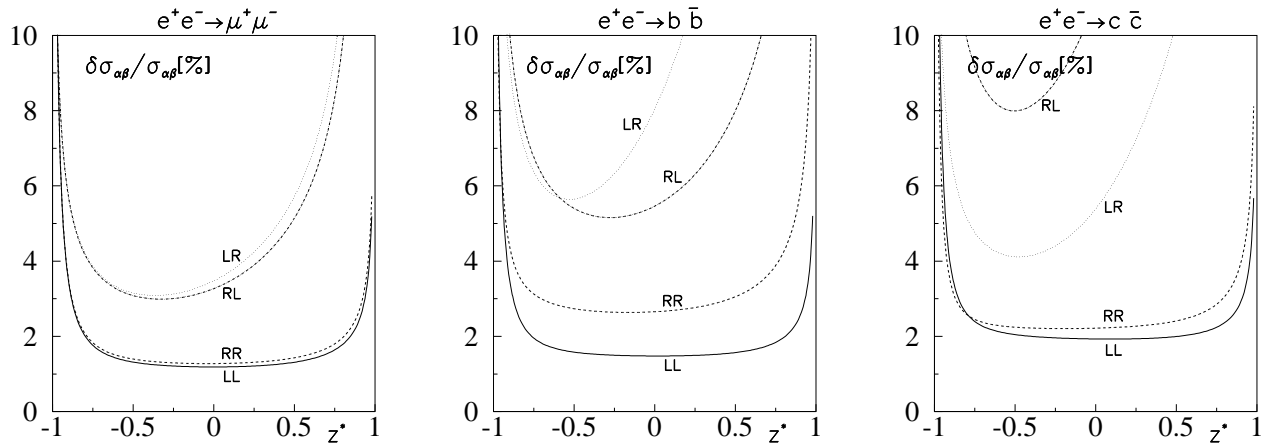


Figure 5: The uncertainty on the helicity cross sections $\sigma_{\alpha\beta}$ in the SM as a function of z^* for the process $e^+e^- \rightarrow \mu^+\mu^-$ at $P_e = 0.9$, $P_{\bar{e}} = 0.6$ and $\sqrt{s} = 0.5 \text{ TeV}$, $\mathcal{L}_{\text{int}} = 50 \text{ fb}^{-1}$.

figures, and in Table 1 we report such z_{opt}^* for the two different values of the luminosity.

Numerical constraints on the four-fermion contact interactions of Eq. (2) are obtained from a χ^2 analysis of data on each helicity cross section, with (see Eq. (21)):

$$\chi^2 = \left(\frac{\Delta\sigma_{\alpha\beta}}{\delta\sigma_{\alpha\beta}} \right)^2. \quad (30)$$

Bounds on the allowed values of the contact interaction parameters from the non-observation of the corresponding deviations within the expected uncertainty $\delta\sigma_{\alpha\beta}$ are derived by imposing $\chi^2 < \chi_{\text{CL}}^2$, where the actual value of χ_{CL}^2 specifies the desired ‘confidence’ level. As Eq. (22) shows, the deviations $\Delta\sigma_{\alpha\beta}$ depend on a single ‘effective’ contact-interaction free parameter, and therefore in such a χ^2 analysis we take $\chi_{\text{CL}}^2 = 3.84$ for 95% C.L. as consistent with a one-parameter fit.

Table 1: Optimal kinematical cut, z_{opt}^* , and resulting contact-interaction reach (in TeV) at 95% C.L. at the LC with $E_{\text{c.m.}} = 0.5$ TeV and double beam polarization: $|P_e| = 0.9$, $(\delta P_e/P_e) = 0.5\%$, $|P_{\bar{e}}| = 0.6$, $(\delta P_{\bar{e}}/P_{\bar{e}}) = 1.0\%$. ($\Lambda_{\alpha\beta}$ values in parentheses refer to no optimization, $z^* = 0$.)

process	\mathcal{L}_{int} [fb ⁻¹]	z^*, Λ_{LL} [TeV]	z^*, Λ_{RR} [TeV]	z^*, Λ_{LR} [TeV]	z^*, Λ_{RL} [TeV]
$\mu^+\mu^-$	50	0.00, (43.0) 43.0	-0.04, (43.4) 43.4	-0.36, (37.7) 40.0	-0.33, (38.6) 40.4
	500	0.50, (54.7) 56.9	0.44, (57.0) 58.8	-0.49, (57.1) 65.5	-0.46, (58.9) 65.7
$b\bar{b}$	50	0.01, (44.8) 44.8	-0.16, (51.0) 51.2	-0.52, (32.9) 39.8	-0.28, (48.2) 49.6
	500	0.57, (50.6) 51.8	0.18, (70.5) 70.7	-0.63, (44.5) 65.0	-0.42, (72.8) 78.7
$c\bar{c}$	50	0.09, (35.6) 35.6	-0.19, (40.1) 40.2	-0.47, (33.6) 38.4	-0.50, (32.0) 37.0
	500	0.60, (38.3) 39.0	0.42, (45.7) 46.0	-0.66, (40.1) 53.5	-0.62, (41.9) 57.9

The results for the bounds on $\Lambda_{\alpha\beta}$ are reported in Table 1. The table shows that the helicity cross sections $\sigma_{\alpha\beta}$ are quite sensitive to contact interactions, with discovery limits that, at the highest considered luminosity 500 fb⁻¹, can range from 75 up to 150 times the c.m. energy, depending on the considered final fermion state. Indeed, the best sensitivity is achieved for the $\mu^+\mu^-$ and $b\bar{b}$ final states, while the worst one corresponds to the $c\bar{c}$ channel. A direct comparison with the sensitivity achieved using ‘conventional’ observables, Eqs. (16)–(20)², is quite difficult and might be unclear, because it depends on the assumed model of new physics involved and the kind of parameterization adopted for the uncertainty. In this regard, as repeatedly stressed, we point out that the separation of the helicity cross sections performed here (and the corresponding values in Table 1) has the qualitative advantage of providing, by definition, unambiguous and model-independent information on the non-standard parameters of Eq. (2).

For a sort of contact to the conventional observables (16)–(20), we have reported in Table 1 also the limits on $\Lambda_{\alpha\beta}$ obtainable at $z^* = 0$ instead of $z^* = z_{\text{opt}}^*$. The results

²See, for example, the results obtained in [15] in the context of specific contact-interaction models.

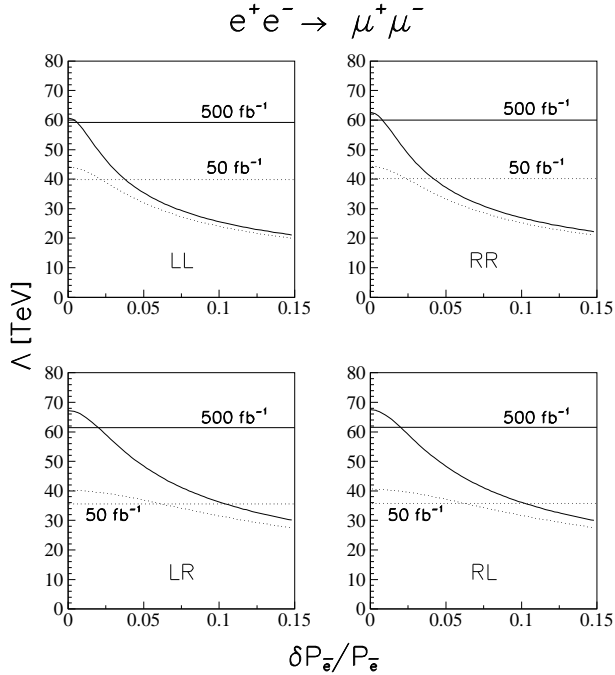


Figure 6: Reach in $\Lambda_{\alpha\beta}$ vs. uncertainty in positron polarization, $\delta P_{\bar{e}}/P_{\bar{e}}$ for $\mu^+\mu^-$ final states. Dashed: 50 fb^{-1} , solid: 500 fb^{-1} . Horizontal lines: no positron polarization.

show that, at $z^* = 0$, the sensitivity to Λ_{LR} and Λ_{RL} would be considerably smaller. As one can see from the table, the ‘optimal’ choice $z^* = z_{\text{opt}}^*$ allows to substantially increase the bounds for the LR and RL cases, to the level of the LL and RR ones, for which the improvement is really modest. This relates to the z^* behavior of the relative uncertainties on $\sigma_{\alpha\beta}$, that, as is seen in Fig. 5, is flat in the latter case and varies more rapidly around z_{opt}^* in the former one.

As discussed previously, and illustrated in Fig. 3, the benefit of positron polarization depends on it being known with some precision. We show in Figs. 6 and 7 the effect of the positron polarization uncertainty on the reach in $\Lambda_{\alpha\beta}$, for the two luminosities considered.

We see from these figures that if the positron polarization is known with high precision, an amount $P_{\bar{e}} = 0.6$ can increase the reach in Λ by typically 5–25%. The critical level of precision, by which the positron polarization should be known, in order to be beneficial for contact-interaction searches, depends very much on the channel considered, as well as the luminosity. At low luminosities, less polarization precision is required for the positron polarization to be useful.

While one polarized beam is a *necessity* in order to be able to extract the helicity cross sections, the benefit of both beams being polarized is less clear. For some combinations of final state and helicity channels, the increased reach in Λ can be considerable, although half luminosity (and correspondingly reduced number of events) has been assumed for the two configurations of electron and positron beam polarizations. However, due to the limiting effect of the polarization uncertainties on the sensitivity (21), such improvements do not seem dramatic. More luminosity might easily lead to the same gain, especially if

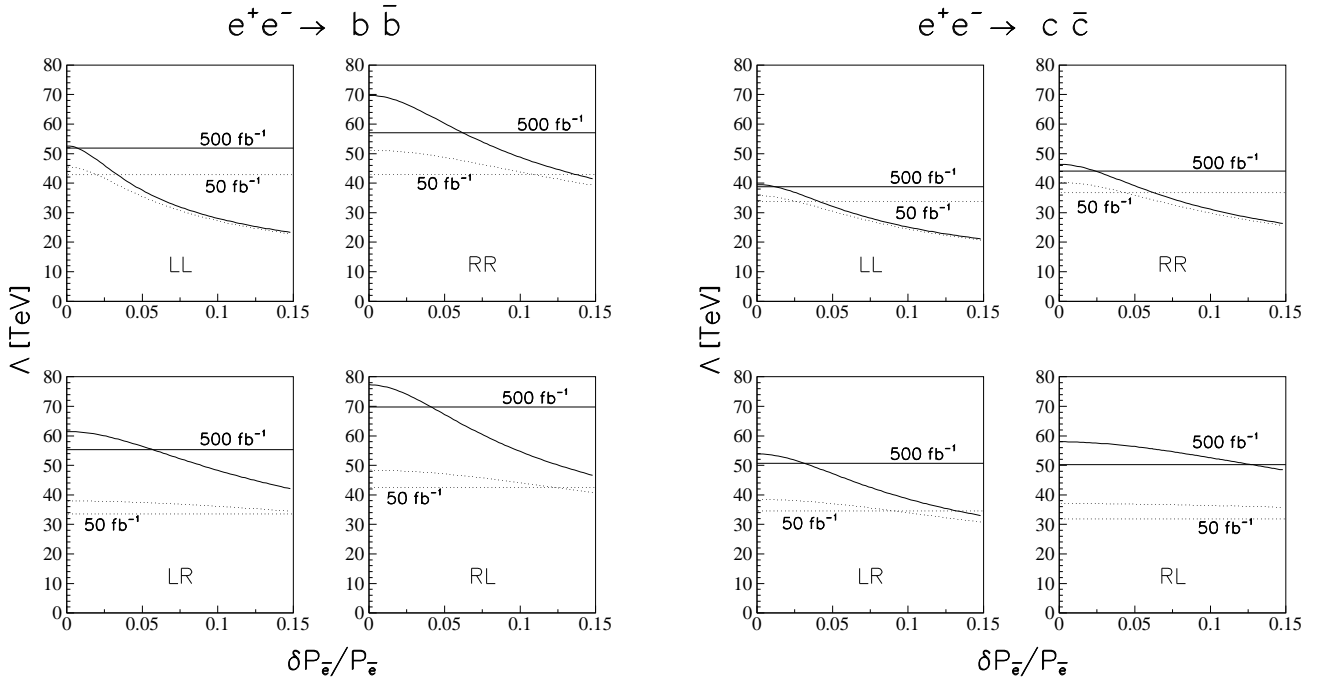


Figure 7: Same as Fig. 6, but for $b\bar{b}$ and $c\bar{c}$ final states.

the positron polarization is only known with a moderate accuracy.

Actually, for full completeness in this regard, the dependence on the actual value of the uncertainty δ^{sys} in (25) should be considered simultaneously with that from $\delta\sigma_{\alpha\beta}^{\text{pol}}$, as suggested by the combination in Eq. (26). Clearly, we should expect reduction of the Λ reach for increasing δ^{sys} . As an indication, by doubling the values of δ^{sys} with respect to those listed below Eq. (25), and adopted for the explicit numerical example presented here, at $\mathcal{L}_{\text{int}} = 50 \text{ fb}^{-1}$ the typical effect amounts to a few percent for the LR and RL cases, but can be as large as 20% for the LL and RR combinations. This indicates that the latter helicity cross sections are much more sensitive to systematic uncertainties than the former ones.

Clearly, although these considerations are numerically drawn from a specific example using as inputs some particular, hypothetical, values of initial beam polarization and corresponding uncertainties, and from assumptions on the values and properties of the uncertainties δ^{sys} of Eq. (25), such conclusions should hold in general. For a definite, quantitative statement about the relative roles of statistical and systematic uncertainties (including δP_e and $\delta P_{\bar{e}}$) in the determination of the accuracy on $\sigma_{\alpha\beta}$ in a realistic experimental situation, we must wait for more detailed information on the expected experimental errors.

References

- [1] E. J. Eichten, K. D. Lane, M. E. Peskin, Phys. Rev. Lett. **50** (1983) 811;
R. Rückl, Phys. Lett. **B 129** (1983) 363.
- [2] V. Barger, K. Cheung, K. Hagiwara, D. Zeppenfeld, Phys. Rev. D **57** (1998) 391;
D. Zeppenfeld, K. Cheung, preprint MADPH-98-1081, hep-ph/9810277.
- [3] G. Altarelli, J. Ellis, G. F. Giudice, S. Lola, M. L. Mangano, Nucl. Phys. **B 506** (1997) 3;
R. Casalbuoni, S. De Curtis, D. Dominici, R. Gatto, Phys. Lett. **B 460** (1999) 135;
V. Barger, K. Cheung, UCD-2000-8, hep-ph/0002259.
- [4] A.A. Babich, P. Osland, A.A. Pankov, N. Paver, Phys. Lett. **B 476** (2000) 95.
- [5] B. Schrempp, F. Schrempp, N. Wermes, D. Zeppenfeld, Nucl. Phys. **B 296** (1988) 1.
- [6] K. Flöttmann, preprint DESY 95-064; K.Fujii, T.Omori, KEK preprint 95-127.
- [7] S. Riemann, FORTRAN program ZEFIT Version 4.2;
D. Bardin et al., preprint DESY 99-070, hep-ph/9908433.
- [8] M. Consoli, W. Hollik, F. Jegerlehner, *in* Z physics at LEP1, G. Altarelli, R. Kleiss, C. Verzegnassi (Eds.), vol.1, p.7, 1989.
- [9] G. Altarelli, R. Casalbuoni, D. Dominici, F. Feruglio, R. Gatto, Nucl. Phys. **B 342** (1990) 15.
- [10] A. Djouadi, A. Leike, T. Riemann, D. Schaile, C. Verzegnassi, Z. Phys. **C 56** (1992) 289.
- [11] See, e.g.: D. Abbaneo et al., The LEP Collaborations, CERN-EP-2000-016;
J. Breitenweg et al., ZEUS Collaboration, DESY-99-058;
C. Adloff et al., H1 Collaboration, DESY-00-027.
- [12] C. J. S. Damerell, D.J. Jackson, in *Proceedings of the 1996 DPF/DPB Summer Study on New Directions for High Energy Physics* (Snowmass 96), Edited by D.G. Cassel, L. Trindle Gennari, R.H. Siemann (SLAC, 1997) p. 442.
- [13] M. Swartz, 19th International Symposium on Lepton and Photon Interactions at High-Energies (LP 99), Stanford, CA, 9-14 Aug 1999.
- [14] E. Accomando et al. (ECFA/DESY LC Physics Working Group), Phys. Rept. **299** (1998) 1.
- [15] S. Riemann, presentation at the “4th International Workshop on Linear Colliders”, Sitges, Spain, 1999.